

Speckle removal in phase reconstruction of digital holography for structured surfaces

Zhang Xiaolei¹, Zhang Xiangchao¹, Xiao Hong², Xu Min¹

(1. Shanghai Engineering Centre of Ultra-Precision Optical Manufacturing, Fudan University, Shanghai 200438, China;

2. Institute of Mechanical Manufacturing Processing, China Academy of Engineering Physics, Mianyang 621999, China)

Abstract: In recent years, digital holographic microscopy has attracted intensive attention for its capability of measuring complex shapes. There are two parts in digital holographic microscopy, hologram recording and digital diffractive reconstruction. Speckles are inevitable in the recorded interferometric patterns, thereby polluting the reconstructed surface topographies. Three reconstruction algorithms, i.e. Fresnel transform, Fresnel-wavelets and the proposed Fresnel-NSCT algorithms were compared. Three typical structures, rectangular, spherical and triangular surfaces were adopted for analysis. The performance of the three reconstruction algorithms on speckle removal and feature preservation was investigated comprehensively. Signal-Noise-Ratio (SNR) and Peak-Signal-Noise-Ratio (PSNR) were used as the numerical criteria. It is found that the Fresnel-NSCT algorithm has great superiority over the other two, subsequently it is promising for applications in the diffractive reconstruction of structured surfaces.

Key words: digital holographic microscopy; structured surface; reconstruction; NSCT; speckle

CLC Number: O438.1 **Document code:** A **DOI:** 10.3788/IRLA201645.0726002

针对结构表面的数字全息相位重构散斑去除方法

张晓磊¹, 张祥朝¹, 肖虹², 徐敏¹

(1. 复旦大学 上海超精密光学制造工程技术研究中心, 上海 200438;

2. 中国工程物理研究院机械制造工艺研究所, 四川 绵阳 621999)

摘要: 近年来, 数字全息显微技术在复杂表面测量领域得到了广泛关注。数字全息技术主要分为干涉记录和重构再现两部分。在激光干涉记录中, 散斑噪声会严重影响测量结果。因此数字全息相位重构的一项重要工作就是去除散斑噪声, 以提高重构精度。分析了带有散斑噪声的几类典型的结构面, 比较了菲涅尔衍射算法、基于小波变换的菲涅尔衍射算法和新提出的基于非下采样轮廓波变换的菲涅尔衍射算法三者散斑去噪和信号保持方面的表现。结果显示: 基于非下采样轮廓波变换的菲涅尔衍射重构算法可以有效提取各类结构面的信息, 有效实现信噪分离。因此, 该方法比现有重构算法可得到更高的重构精度, 在结构表面的相位重构方面具有重要应用价值。

关键词: 数字全息显微; 结构表面; 重构; 非下采样轮廓波变换; 散斑

收稿日期: 2015-11-05; 修订日期: 2015-12-03

基金项目: 国家自然科学基金(51205064); 上海市自然科学基金(12ZR1441100); 中国工程物理研究院开放基金(KF14004)

作者简介: 张晓磊(1990-), 男, 博士生, 主要从事数字全息显微技术方面的研究。Email: 13110720008@fudan.edu.cn

导师简介: 张祥朝(1982-), 男, 副研究员, 博士, 主要从事光学检测技术及表面计量方面的研究。Email: zxchao@fudan.edu.cn

0 Introduction

Structured surfaces contain salient structures designed to provide a specular function. While these structures and surface features are becoming smaller, accurate measurement of their surface topographies turns out to be an important issue. Subsequently various measuring methods, including stylus profilometry and optical profilometry have been developed^[1-2]. But the former technology like AFM and SPM is likely to damage structured surfaces. And the latter like phase shifting interferometry, confocal microscopy and white-light interferometry have some problems in limited measuring range and capability of measuring complex shapes.

Digital holography is of great advantage not only for its high-sensitivity, high accuracy, high resolution, fast capture, and nondestructive measurement^[3], but also due to its convenience and flexibility to implement, as a result it obtains worldwide application in the fields of biomedicine^[4-5], MEMS^[6], micro optics^[7] and so on. An essential technique in digital holography is reconstruction of the measured wavefronts from the interferometric patterns of holograms. There are three reconstruction algorithms commonly used, Fresnel diffraction integration, Somerfield diffraction integration and angular spectrum method. However during the process of hologram recording, speckle noise is inevitable^[8], thus denoising is an important part of the reconstruction algorithm. In the last decade, multi-resolution (MR) methods have been applied in image denoising. One of the most widely used analysis tools is wavelets^[9]. Due to the limited number of directions, wavelets have poor-performance for line or curve singularities. While directional features like edges, steps, and grooves are the dominant morphologies of structured surfaces, hence wavelets are not suitable to be used in the holographic reconstruction of structured surfaces.

1 Methodology

1.1 Typical reconstruction algorithms

1.1.1 Fresnel diffraction integration

According to the theory of Fresnel diffraction, the complex amplitude distribution of the reconstruction field is:

$$U(x_i, y_i, z_i) = \exp\left[\frac{jk}{2z_i}(x_i^2 + y_i^2)\right] F\{C(x, y)H(x, y) \times \exp\left[\frac{jk}{2z_i}(x^2 + y^2)\right]\} \Big|_{f_x = \frac{x_i}{\lambda z_i}, f_y = \frac{y_i}{\lambda z_i}} \quad (1)$$

$C(x, y)$ is the complex amplitude distribution of the reference wave, z indicates the reconstruction distance, $H(x, y)$ indicates the distribution function of the hologram intensity, $F\{\}$ refers to 2-D Fast Fourier Transform (FFT) in the digital reconstruction.

The intensity of recorded hologram is as follows:

$$H(k\Delta x, l\Delta y) = H(x, y) \text{rect}\left(\frac{x}{M\Delta x}, \frac{y}{M\Delta y}\right) \times \sum_k \sum_l \delta(x - k\Delta x, y - l\Delta y) \quad (2)$$

M and N refer to the numbers of image elements in the horizontal direction and vertical direction respectively. Δx and Δy denote the corresponding sizes of image elements. k and l are integers with $-M/2 \leq k \leq M/2 - 1$, $-N/2 \leq l \leq N/2 - 1$. The integration effects involved in the CCD sampling have been omitted here.

The reconstruction distance should satisfy the following condition:

$$z \geq \left\{ \frac{\pi}{4\lambda} \left[\left(\frac{L_x}{2} + \frac{M\Delta x}{2} \right)^2 + \left(\frac{L_y}{2} + \frac{N\Delta y}{2} \right)^2 \right] \right\}^{1/3}$$

L_x and L_y are the extent in x and y directions.

1.1.2 Convolution reconstruction algorithm

Convolution reconstruction algorithm can be described as:

$$U(x_i, y_i, z_i) = F^{-1}\{F[C(x, y)H(x, y)] \cdot F[g(x, y)]\} \quad (3)$$

$F^{-1}\{\}$ denotes the 2-D inverse Fourier transform, $g(x, y)$ is the impulse response of free space as follows:

$$g(x, y) = \frac{1}{j\lambda} \frac{\exp[jk(z_i^2 + x^2 + y^2)^{1/2}]}{(z_i^2 + x^2 + y^2)^{1/2}}$$

The complete convolution reconstruction algorithm needs to implement FFT three times. Here $g(k\Delta x, l\Delta y)$ is used to denote the discrete impulse response. The transform function is:

$$G_{CV}=(m\Delta f_x, n\Delta f_y)=\text{FFT}\{g(k\Delta x, l\Delta y)\} \quad (4)$$

with $-M/2 \leq k \leq M/2-1$, $-N/2 \leq l \leq N/2-1$ and $\Delta f_x = \frac{\Delta x_i}{\lambda z_i}$,

$\Delta f_y = \frac{\Delta y_i}{\lambda z_i}$. According to the Nyquist sampling theorem

$2f_{x\max} \leq 1/\Delta x$, $2f_{y\max} \leq 1/\Delta y$ the reconstruction distance

should meet the condition $z_i \geq \max\left(\frac{M\Delta x_i}{\lambda}, \frac{M\Delta y_i}{\lambda}\right)$.

1.1.3 Angular reconstruction algorithm

According to the angular spectrum theory, the distribution of complex amplitude of the reconstruction image is described as^[10]:

$$U(x_i, y_i, z_i) = F^{-1}\{F[C(x, y)H(x, y)] \cdot G_{AS}(f_x, f_y)\} \quad (5)$$

with: $G_{AS}(f_x, f_y) = \exp[jkz\sqrt{1-(\lambda f_x)^2-(\lambda f_y)^2}]$

Here $G_{AS}(f_x, f_y)$ is the transfer function.

It has been proved that there will be no limitation on the reconstruction distance when using the Fresnel transform reconstruction algorithm. The convolution reconstruction algorithm can obtain high resolution images in a very limited extent near the optimum reconstruction distance. While the angular spectrum algorithm can obtain high resolution image at a large extent of reconstruction distance around the optimum reconstruction distance. Thus the Fresnel transform algorithm is preferable for its simplicity, efficiency and greater range of reconstruction distance.

1.2 Multi-resolution (MR) methods

Speckle noise is inevitably added into this holograms in the laser recording system. The recorded hologram is the sum of original data and zero-mean speckle noise. Denoising can be carried out by transforming noisy data into the transform domain like wavelets, curvelets and contourlets, identifying noise by thresholding, and then reconstructing the denoised data. Confined to the length of the paper, the wavelets and contourlets transforms are presented briefly.

1.2.1 Wavelets

Wavelets are an efficient tool to isolate the discontinuities at point-like features. There are two spaces as a projection of a discrete signal, the approximation space Φ and a series of detail (wavelet) spaces Ψ . The projection is obtained by discrete time sub-band decomposition of the input signal by filtering

$$\Phi(t) = \sum_n h_0(-n)\sqrt{2} \phi(2t-n)$$

$$\Psi(t) = \sum_n h_1(-n)\sqrt{2} \varphi(2t-n) \quad (6)$$

where $h_0(n)$ is a low-pass filter while $h_1(n)$ is a high-pass filter associated with the wavelet function $\Phi(t)$ and $\Psi(t)$, respectively. The decomposition for a 2D signal corresponds to projecting the input signal f into four subspaces.

Wavefronts of structured surfaces have apparent directional contours. However wavelets extract directional information only from the limited three directions, horizontal, vertical and diagonal, thus they are not well adapted to complex edge- singularity.

1.2.2 Non-subsampled contourlet transform

Non-subsampled contourlet transform (NSCT)^[11], based on the theory of contourlet, can capture directional details and smooth anisotropy contours, and it also possess a superiority of shift-invariance over the conventional contourlet transform. NSCT is based on the non-subsampled pyramid (NSP) and non-subsampled directional filter banks(NSDFB). The brief implementation procedure of NSCT is shown in Fig.1.

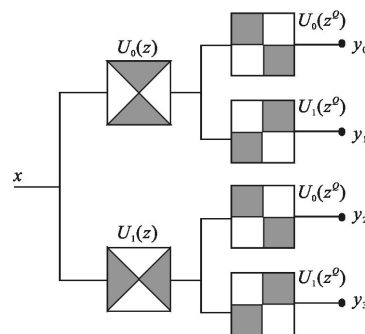
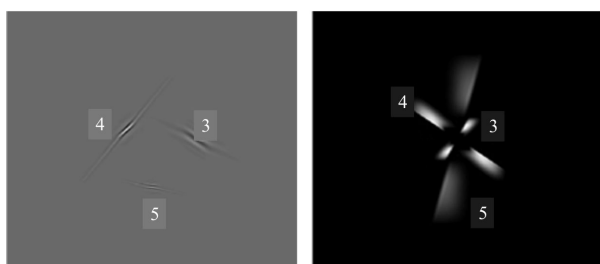


Fig.1 Schematic structure of NSCT

NSCT makes it possible to obtain the geometrical features at any scale and along any direction. The same as wavelets, NSCT has a space-frequency localization property. Fig.2(a) is the spatial representation, while Fig.2(b) is the magnitude of the Fourier frequency representation. The coarse-scale in spatial domain corresponds to shorter side in frequency domain, implying that low spatial resolution corresponds to high frequency resolution.



(a) Spatial domain (b) Frequency domain

Fig.2 NSCT basis function

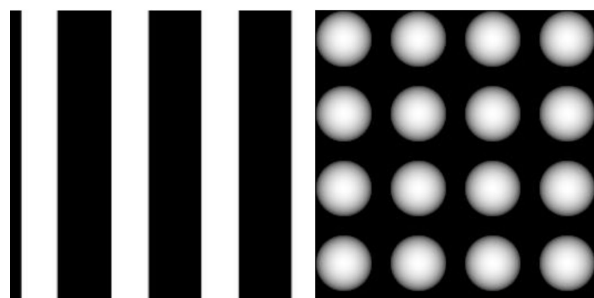
The characteristics of the surface morphologies determine the number of decomposed directions. Structured surfaces have sparse representations in the domain of NSCT, while speckles spread in a lot of terms, subsequently they can be removed straightforwardly by thresholding.

2 Simulation and Experiment

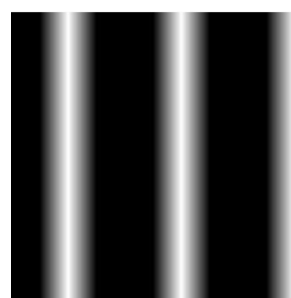
2.1 Simulation: three typical reconstruction

A typical reconstruction algorithm, the Fresnel reconstruction algorithm, and two MR methods, Fresnel algorithm with wavelets (Fresnel-wavelets) and Fresnel algorithm with NSCT (Fresnel-NSCT), are compared by revealing the difference between the original data and the denoised data. Signal-Noise-Ratio (SNR) and Peak-Signal-Noise-Ratio (PSNR) are used as the numerical criteria to estimate the performances of three reconstruction algorithms. The peaks and valleys (PV) values and root-mean-square (RMS) values of the residual noise are also provided. Noise added to the original image is all supposed to be zero-mean speckle noise with the standard deviation $\sigma = 0.3$. Three typical structured surfaces (Fig.3): rectangular, triangular and spheroidal surfaces are

employed.



(a) Rectangular (b) Spheroidal



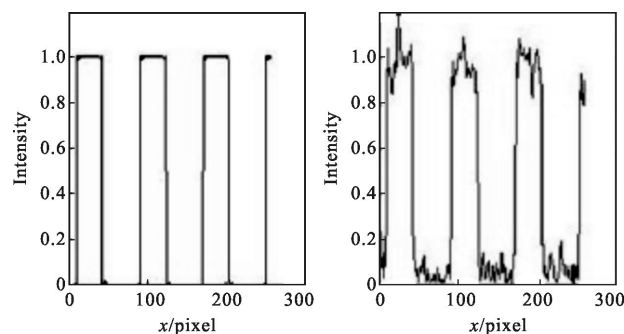
(c) Triangular

Fig.3 Typical structured surfaces

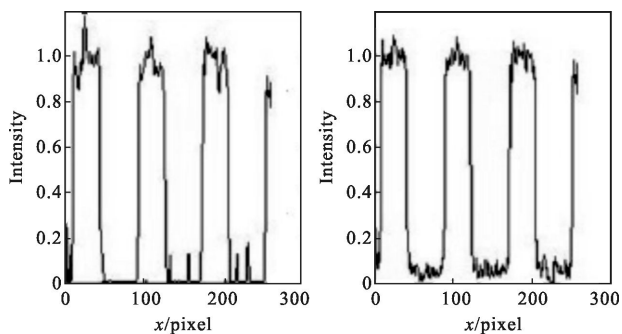
2.1.1 Rectangular

A numerical example is presented here for the feature decomposition of structured surfaces. The size of the data set is 256×256 . The diffraction distance is 100 mm, the diffraction window is $50 \text{ mm} \times 50 \text{ mm}$ and the wavelength applied is 632.8 nm. A cross section is presented in Fig.4 to expose the denoising ability both on the edges and on the structures of each reconstructed surface.

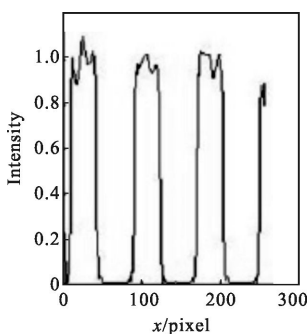
Fresnel reconstruction algorithm retains remarkable noise along the contours and the contaminated signals on the structured surfaces are maintained as shown in the cross section.



(a) Original (b) Noisy



(c) Denoised by Fresnel (d) Denoised by Fresnel-wavelets



(e) Denoised by Fresnel-NSCT

Fig.4 A cross section of the rectangular structured surface

Since its PV value of the residual speckles is ranked the maximum in Tab.1, this algorithm removes only low-value noise. As for Fresnel-wavelets, obviously the speckle noise, which is along with a

Tab.1 Numerical results of three reconstruction algorithms

	Surfaces	SNR/PSNR	PV/RMS (Residual)	Time/s
Fresnel	Rectangular	17.6304/69.6840	0.9501/0.0836	0.11
	Triangular	18.0799/73.6538	0.6723/0.0529	
	Spheroidal	20.0857/74.4204	0.6504/0.0485	
Fresnel-wavelets	Rectangular	17.0411/69.0946	0.7820/0.0895	0.24
	Triangular	17.7636/73.3374	0.5741/0.0549	
	Spheroidal	13.6365/67.9707	1.5278/0.1019	
Fresnel-NSCT	Rectangular	18.5661/70.6197	0.8884/0.0751	3.46
	Triangular	20.9877/76.5616	0.5832/0.0379	
	Spheroidal	22.5650/76.8952	0.5812/0.0365	

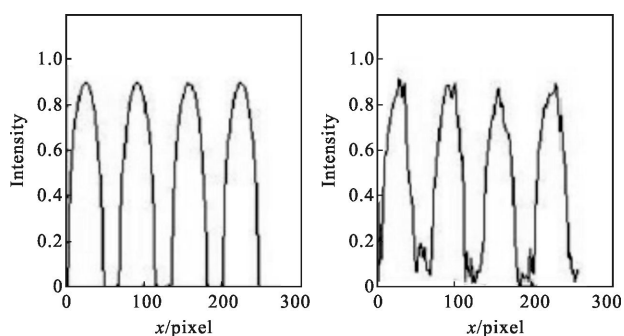
little noise on the edge of each rectangle, has been declined. With the minimum PV and RMS values of the remanent noise, Fresnel-wavelets has great ability in reducing the noise but is not able to smooth the structures, as proved by Fig.4(d). On the contrary, Fresnel-NSCT algorithm has attractive performance along the

contours. Both of the minimum RMS value and Fig.4(e) demonstrate that NSCT could smooth the step surface with higher fluctuation than that in Fig.4(d).

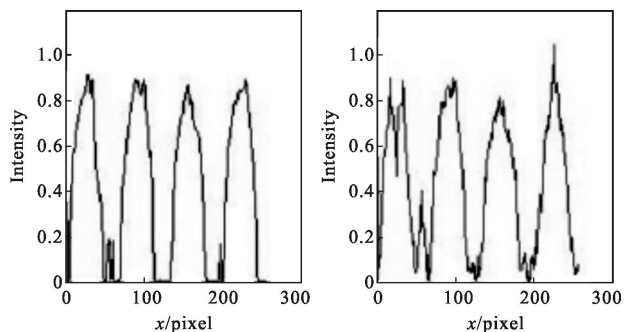
2.1.2 Spheroidal

With the same parameters of the simulative rectangular structures, spheroidal structures are emulated as the structured surface.

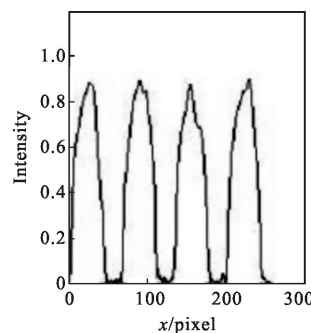
Similar to steps, Fresnel algorithm is helpless to eliminate large speckles as shown in Fig.5(c). Fresnel-wavelets is undisputedly the worst reconstruction



(a) Original (b) Noisy



(c) Denoised by Fresnel (d) Denoised by Fresnel-wavelets



(e) Denoised by Fresnel-NSCT

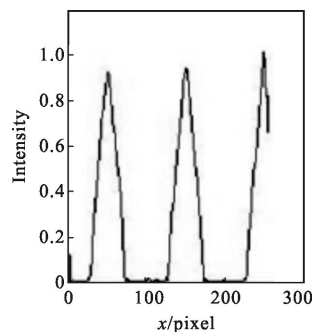
Fig.5 A cross section of the spheroidal structured surface

algorithm for it has changed the original signals. As mentioned before, wavelets have only three directions so that signals will be reconstructed into rectangles after thresholding instead of retaining curves. While the speckle noise between hemi-spheres has almost been removed completely, Fresnel-NSCT owns the best reconstruction ability. Figure 5 has also testified the results that Fresnel-NSCT is a proper choice for its capacity of smoothing structured surfaces and denoising along the contours.

2.1.3 Triangular

The last surface is triangular adopting the same parameters. Three sets of images are given to exhibit the features on the reconstructed surface, the reconstructed images using three reconstruction algorithms, a cross section and a vertical section of each reconstructed surface as depicted in Fig.6 and Fig.7.

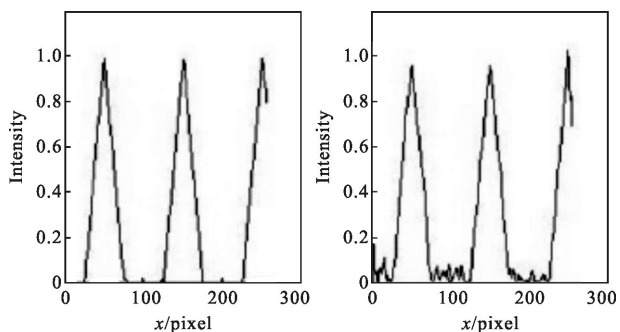
The speckle noise left on the surface and along the contours shown in Fig.6(c) and Fig.7(a) have already changed the shape of structures, especially on the edges, thus Fresnel algorithm is not suitable for this surface. Because of the structure is along the



(e) Denoised by Fresnel-NSCT

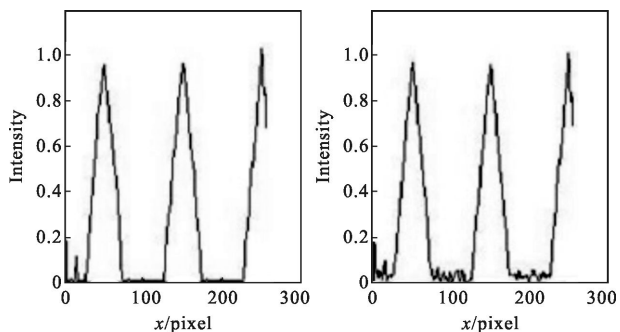
Fig.6 A cross section of the triangular structured surface

vertical direction, Fresnel-wavelets removes most speckle noise inside each triangle. Combined with the cross section (Fig.6(d) and Fig.6(e)) and the vertical section of reconstructed surfaces(Fig.7(b) and Fig.7(c)) using wavelets and NSCT, it is found that NSCT would not only smooth signals inside structured surface but also be able to reduce its fluctuation. Eliminating much more noise on the surface and retaining shapes more completely of the original signals, NSCT is proved superior to wavelets for triangular structured surfaces.



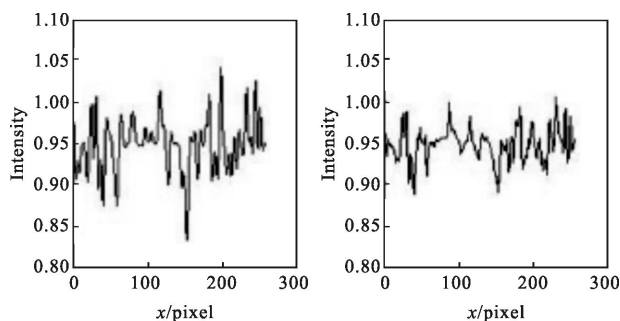
(a) Original

(b) Noisy



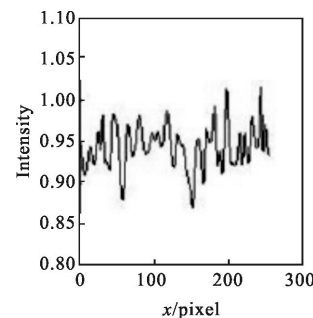
(c) Denoised by Fresnel

(d) Denoised by Fresnel-wavelets



(a) Denoised by Fresnel

(b) Denoised by Fresnel-wavelets



(c) Denoised by Fresnel-NSCT

Fig.7 A vertical section of the triangular reconstructed surface

The numerical result is listed in Tab.1. It shows that Fresnel algorithm has the fastest speed, while Fresnel-NSCT has the best SNR and PSNR values. Fresnel-wavelets acquires good results in rectangular and triangular structured surfaces.

2.2 Hologram reconstruction

In this section, true holographic data is recorded using an in-line geometry. An object was illuminated using a He-Ne laser($\lambda=632.8$). The reflected wave was then directed to the 1024×1024 pixels CCD camera. The phase of object wave was obtained by four-step phase shifting using PZT. The sampling step of the CCD was 5 μm and diffraction distance was 50 mm.

Figure 8 demonstrated the conclusion in Section 2.1. Overall the Fresnel algorithm cannot recognize directional components, thus it cannot separate noise from signals. That is the reason why it will leave conspicuous speckles in the reconstruction images when using a small threshold and destruct signals when using a large threshold. Fresnel-wavelets would decompose signals into three directions so that it has poor capability to reconstruct the contours, and the

curved features can be destructed. On the contrast, Fresnel-NSCT algorithm has excellent denoising performance for non-smooth structured surfaces. As contours between piecewise continuous sections have sparse representations after contourlet transform, then speckles can be recognized and removed straightforwardly in the transform domain.

3 Conclusions

In this paper, a typical reconstruction algorithm Fresnel, and the MR reconstruction algorithms, Fresnel-wavelets and the proposed Fresnel-NSCT, are compared for structured surfaces. Unfortunately, the commonly-used Fresnel reconstruction algorithm has little efficiency for reconstruction of structured surfaces, and the speckles and noise cannot be removed effectively. Possessing outstanding effectiveness to represent point singular signals, the Fresnel-wavelets algorithm work well for steps and triangles. However it cannot deal with curves. At the cost of complexity, the Fresnel with NSCT reconstruction algorithm proposed in this paper owns the best competence to reduce speckle noises and preserve features for non-smooth structured surfaces.

References:

- [1] Zhou Mingbao, Lin Dajian, Gou Lurong, et al. Measurement of micro structure surface topography [J]. *Optics and Precision Engineering*, 1999, 7(3): 7-13. (in Chinese)
- [2] Conroy M, Armstrong J. A comparison of surface metrology techniques [C]//Journal of Physics Conference Series, 2006: 458-465.
- [3] Zhou Hao, Gu Jihua, Chen Daqing. Multi-plane imaging in digital holography [J]. *Infrared and Laser Engineering*, 2015, 44(2): 513-518. (in Chinese)
- [4] Moon I, Yi F, Rappaz B. Automated tracking of temporal displacements of a red blood cell obtained by time-lapse digital holographic microscopy [J]. *Applied Optics*, 2016, 55(3): 1670-1674.
- [5] Zhou Minghui, Liao Chunyan, Ren Zhaoyu, et al. Bioimaging technologies based on surface-enhanced Raman spectroscopy and their applications[J]. *Chinese Optics*, 2013,

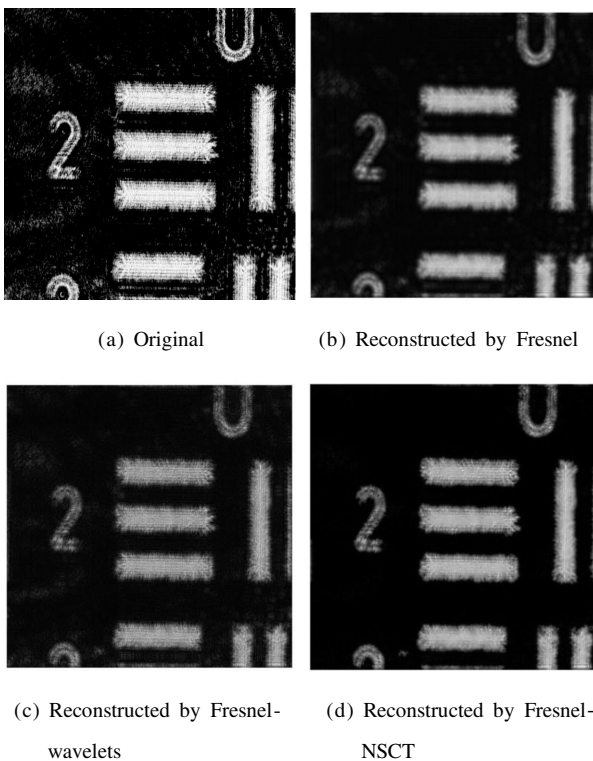


Fig.8 Experiment results

- 6(5): 633–642. (in Chinese)
- [6] Udupa G, Ngoi B K A, Goh H C F, et al. Defect detection in unpolished Si wafers by digital shearography [J]. *Measurement Science & Technology*, 2004, 15(1): 35–43.
- [7] Henderson V A, Griffin P F, Riis E, et al. Comparative simulations of Fresnel holography methods for atomic waveguides[J]. *New Journal of Physics*, 2016, 18(2).
- [8] Wu Kun, Zhang Hexin, Meng Fei, et al. Denoising method of intensity image for laser active imaging system [J]. *Infrared and Laser Engineering*, 2013, 42(9): 2397–2402. (in Chinese)
- [9] Kong Qingnan, Wang Shande, Zhang Chi, et al. Influence of laser speckle average size on ghost imaging [J]. *Optics and Precision Engineering*, 2015, 23(10z): 198–204. (in Chinese)
- [10] Salau J, Haas J H, Thaller G, et al. Developing a multi-Kinect-system for monitoring in dairy cows: object recognition and surface analysis using wavelets.[J]. *Animal*, 2016, 1: 1–12.